Energy Harvesting Relaying Network in a Delay-Tolerant Transmission Mode Over κ—μ Shadowed Fading Channels

Ayaz Hussain†, Inayat Ali †, Zahoor Ahmed †, and Sang-Hyo Kim ††

†Department of Electrical Engineering, Balochistan University of Engineering and Technology, Khuzdar, Pakistan.
††College of Information and Communication Engineering, Sungkyunkwan University, Suwon, South Korea.

Summary
Here, energy harvesting DF (decode-and-forward) relaying with beamforming is studied in $\kappa-\mu$ fading environment. In this system, a source and a destination are equipped with multiple antennas, and communication from the source to the destination takes place via a single antenna DF relay. The relay is an energy-constrained node and harvests energy from the received source RF (radio-frequency) signal. Then, using the harvested energy, the relay transmits information to the destination. The $\kappa-\mu$ shadowed fading includes different classical fading models as distinctive cases: Rayleigh, Nakagami-$\hat{m}$, $\kappa-\mu$, Rician, and Rician shadowed fading. Using a PSR (power-splitting relaying) protocol, new and exact analytical expressions for the average capacity and throughput are derived in a delay-tolerant transmission mode. The system performance is analyzed for different number of antennas in different fading and shadowing environment. The derived analytical results are justified through Monte Carlo simulation.

Key words:
Energy harvesting, decode-and-forward relay, $\kappa-\mu$ shadowed fading, power-splitting-based relaying, throughput.

1. Introduction

Wireless energy harvesting is a process to extract energy from radio frequency (RF) signals, and has been proposed as an emerging solution to extend the lifetime of wireless networks [1-14]. RF signals can carry both energy and information simultaneously [1], therefore, using an RF-based energy harvesting technique, energy can be harvested from the ambient RF signals and can be stored in a rechargeable battery [1].

Wireless energy harvesting in a dual-hop relaying is an important application and has been extensively investigated [4-14]. In a dual-hop relaying, an intermediate node (i.e., relay) receives information signals from the source node and forwards it to the destination node [2]. There are two main kinds of relaying techniques: amplify-and-forward (AF) and decode-and-forward (DF) relaying. In a DF relaying technique, relay decodes the received signal from the source and forwards it to the destination after encoding it [5]. Recently, wireless energy harvesting in a DF relaying technique received much interest [4-14]. For a dual-hop relaying, there are two main energy harvesting protocols in the literature: time-switching-based relaying (TSR) and power-splitting-based relaying (PSR) protocol [4]. In a TSR protocol, time is divided alternatively between the energy harvesting and information processing at the relay. In a PSR protocol, the received power at the relay is divided into two parts, one part is utilized for the information processing and second part is utilized for the energy harvesting [4].

A single antenna source has a lower efficiency to transfer wireless energy towards a destination, as the RF signals propagates from the single antenna source in all directions, therefore, signals can heavily be affected by shadowing, fading, and path loss before reaching to the receiver [5]. Multi-antenna beamforming techniques have greater efficiency to combat the shadowing, fading, and path loss, and are used to transfer the energy towards the receiver in a narrow beam to increase the signal gain [5]. In a relaying system, utilizing beamforming techniques at the source and destination, can enhance the system capacity and overall quality of the links [5] [15].

Wireless energy harvesting in a dual-hop DF relaying networks has been studied in several works. In [6], throughput performance was analyzed of a DF relaying system over Rayleigh fading channels for PSR and TSR protocols. Wireless energy harvesting relaying with an interference-aided scheme is studied for Rayleigh fading chanels in [7]. In [8], a dynamic DF relaying network for energy harvesting is investigated and the system performance is analyzed for the outage probability under Rayleigh fading environments. In order to increase the diversity gain in a dual-hop energy harvesting relaying, in [9], authors investigated the relay selection schemes, where the system performance was analyzed in terms of outage probability for non-identical Rayleigh fading channels. In [10], the outage and diversity performances of simultaneous wireless information and power transfer in DF cooperative networks with spatially random relays have been investigated for Rayleigh fading channels. This work was extended in [11] for relay selection where the relays have storage devices and they forward the data to the destination when are fully charged by the received RF signals. In [12], partial relay selection protocol using DF non-linear energy harvesting is studied. In [13], energy harvesting in DF relaying system is investigated in mixed $\kappa-\mu$ and $\eta-\mu$ fading environment, where approximate

Manuscript received March 5, 2018
Manuscript revised March 20, 2018

expressions for the outage probability, throughput, and bit-error rate are derived. Recently, in [14], an energy harvesting dual-hop relaying system with beamforming is studied for κ − μ shadowed fading channels, where the outage probability and throughput expressions are derived in a delay-limited transmission mode, and system performance is analyzed for different fading and shadowing parameters.

In the above mentioned work [14], an energy harvesting dual-hop relaying network is studied in a delay-limited transmission mode, and outage probability and throughput performance was analyzed in a κ − μ shadowed fading environment. Despite the importance of a delay-tolerant transmission mode in a dual-hop energy harvesting relaying network, the system performance is not analyzed over κ − μ shadowed fading channels.

In this paper, we consider a DF relaying network where a multi-antenna source is communicating with a multi-antenna destination via a single-antenna relay. It is assumed that the relay is an energy-constrained node which harvests energy from the received source signal. Considering a power splitting-based relaying approach [4], we analyze the system performance over κ − μ shadowed fading channels. First, we derive the exact analytical expressions for the average capacity and throughput in a delay-tolerant transmission mode. In the delay-tolerant transmission mode, a receiver can buffer the received information blocks and can tolerate the delay in decoding the received signal [4]. Then, using the derived analytical results, we analyze the system performance under κ − μ shadowed fading environment for various scenarios at different system parameters, such as, power splitting ratio, number of antennas, noise variances, distances between source-relay and relay-destination, and fading and shadowing parameters. It is worth to note that the κ − μ scenario is general and can be specialized to some particular cases such as Rayleigh/Rayleigh, Nakagami-$\hat{m}$/Nakagami-$\hat{m}$, Rician/Rician, Rician shadowed/Rician shadowed, and mixed κ − μ shadowed, κ − μ, Rician shadowed, Rician, Nakagami-$\hat{m}$, and Rayleigh fading links.

This paper is arranged as follows: The system and channel models for an energy harvesting DF relaying network is described in Section 1. In Section 2, exact analytical expressions for the average capacity and throughput are obtained. Special cases are discussed in Section 4. Section 5 presents the numerical results. In the last, Section 6 concludes this paper.

2. System and Channel Models

2.1 System Model

A three node relaying network is considered, where a single antenna relay R helps a source S to communicate with a destination D. The source and the destination have multiple antennas, N_1 and N_2, respectively. There is no direct communication from the source to the destination and all nodes know the CSI (channel state information). We consider a PSR receiver [4] at the relay node R, where a power splitter splits the received signal in $\rho:1-\rho$ proportion where $\rho \in (0,1)$ is the power splitting ratio [4]. For information processing and energy harvesting at node R, the transmission block structure R, is shown in Fig. 1 [4],

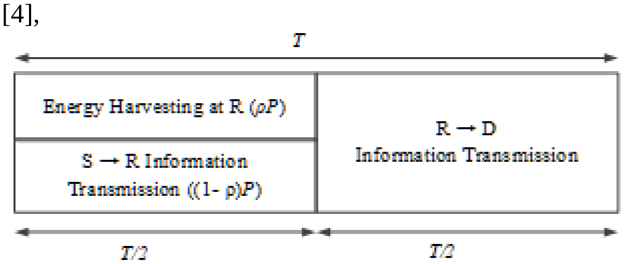

Fig. 1 Transmission block structure of the PSR protocol at node R.

herein, P is the received power at R from the source, T is the block time for a block of information between S and D. The block length is divided into two sessions. Using MRT (maximum-ratio transmission) technique [5], the source sends energy and information to the relay in the first session, in which a portion of the received power ρP is utilized to harvest energy, and other power portion $(1-\rho)P$ is utilized to process the information signal. Using the harvested energy, R forwards its decoded information to D. The destination combines all received signals employing MRC (maximum-ratio combining) technique. The received signal at the node R is given by [5]

$$y_R = \frac{1}{\sqrt{d_1^{\alpha}}}\sqrt{P_s}\mathbf{h}_1^{\dagger} w_1 x + n_{a,r} \quad (1)$$

where $(\cdot)^{\dagger}$ denotes the conjugate transpose, $\|\cdot\|$ shows the Euclidean norm, P_s designates the transmit power of the source, $\mathbf{h}_1$ shows the $N_1 \times 1$ channel vector between the source and relay, x is the normalized source information signal, $w_1 = \frac{\mathbf{h}_1}{\|\mathbf{h}_1\|}$ [5], d_1 is the distance between S and R, α is the path-loss exponent, and $n_{a,r}: (0,\sigma_{a,r}^2)$ is the AWGN (additive white Gaussian noise) at R. Using the

PSR protocol, the relay node R divides y_R into two portions: One portion $\sqrt{\rho}y_R$ is utilized to harvest energy by the energy harvesting receiver, and the second portion $\sqrt{1-\rho}y_R$ is used to process the information by the information receiver. During $T/2$, the energy harvesting receiver harvests the energy at node R as [5]

$$E_h = \frac{\eta\rho P_s \|\mathbf{h}_1\|^2}{d_1^{\alpha}}(T/2), \tag{2}$$

where $0 \le \eta \le 1$ shows the energy conversion efficiency. Subsequently, the relay transmit power P_r can be written by

$$P_r = \frac{E_h}{T/2} = \frac{\eta\rho P_s \|\mathbf{h}_1\|^2}{d_1^{\alpha}}. \tag{3}$$

At the information receiver, the second portion of the received signal $\sqrt{1-\rho}y_R$, is written by

$$\sqrt{1-\rho}y_R = \frac{1}{\sqrt{d_1^{\alpha}}}\sqrt{(1-\rho)P_s}\mathbf{h}_1^{\dagger}\mathbf{w}_1 x + \sqrt{(1-\rho)}n_{a,r} + n_{c,r}, \tag{4}$$

where $n_{c,r} : (0,\sigma_{c,r}^2)$ represents the AWGN at the relay node. Then, using (4), the signal-to-noise ratio (SNR) at the relay node can be given by

$$\gamma_R = \frac{P_s \|\mathbf{h}_1\|^2 d_1^{-\alpha}(1-\rho)}{(1-\rho)\sigma_{a,r}^2 + \sigma_{c,r}^2}. \tag{5}$$

Using the harvested power, P_r, the relay decodes and forwards the information signal (4) to the destination. At the destination, the received signal is given by

$$\mathbf{y}_D = \frac{1}{\sqrt{d_1^{\alpha}d_2^{\alpha}}}\sqrt{\eta\rho P_s \|\mathbf{h}_1\|^2}\mathbf{h}_2^{\dagger}\mathbf{w}_2 x_r + \mathbf{n}_{a,d} + \mathbf{n}_{c,d} \tag{6}$$

where $\mathbf{w}_2 = \frac{\mathbf{h}_2}{\|\mathbf{h}_2\|}$ [15], $\mathbf{h}_2$ is the $1\times N_2$ channel vector between R and D, x_r represents the transmitted signal from the relay, d_2 indicates the distance between R and D, $\mathbf{n}_{a,d} : (0,\sigma_{a,d}^2\mathbf{I}_{N_2})$ and $\mathbf{n}_{c,d} : (0,\sigma_{c,d}^2\mathbf{I}_{N_2})$ are the AWGNs at the antennas and RF-to-baseband conversion, respectively, at D. The SNR at the destination γ_D is given as

$$\gamma_D = \frac{\eta\rho P_s \|\mathbf{h}_1\|^2\|\mathbf{h}_2\|^2}{d_1^{\alpha}d_2^{\alpha}(\sigma_{a,d}^2 + \sigma_{c,d}^2)}. \tag{7}$$

2.2 Channel Model

The κ − μ shadowed fading is a general fading model and comprises effects of fading and shadowing simultaneously [16]. If any link of the dual-hop relaying network experiences κ − μ shadowed fading, then, the channel-power gain $\|h_\ell\|^2$ ($\ell = 1,2$) can be considered as a κ − μ shadowed distributed with mean λ_ℓ. The parameter κ_ℓ is the dominant component to the scattered-waves power ratio and μ_ℓ is a number of clusters. The PDF (probability density function) of the $\ell-th$ link can be given by [15, eq. (3)]

$$f_{\|h_\ell\|^2}(\gamma) = \underbrace{\left(\frac{\mu_\ell(1+\kappa_\ell)}{\lambda_\ell}\right)^{N_\ell\mu_\ell}\left(\frac{m_\ell}{m_\ell+\kappa_\ell\mu_\ell}\right)^{N_\ell m_\ell}}_{\triangleq\xi_\ell} \times \frac{1}{\Gamma(N_\ell\mu_\ell)}\gamma^{N_\ell\mu_\ell-1}\exp\left(-\underbrace{\frac{\mu_\ell(1+\kappa_\ell)}{\lambda_\ell}}_{\triangleq\psi_\ell}\gamma\right) \times {}_1F_1\left(N_\ell m_\ell; N_\ell\mu_\ell; \underbrace{\frac{\kappa_\ell\mu_\ell^2(1+\kappa_\ell)}{(m_\ell+\kappa_\ell\mu_\ell)\lambda_\ell}}_{\triangleq\delta_\ell}\gamma\right), \tag{8}$$

where m_ℓ and $\Gamma(\cdot)$ represent the shadowing parameter and the Gamma function, respectively, ${}_1F_1(\cdot;\cdot;\cdot)$ is the confluent hypergeometric function [17] and which can be written in a summation form as ${}_1F_1(a;b;z) = \sum_{n=0}^{\infty}\frac{(a)_n z^n}{n!(b)_n}$ [17, eq. (9.210.1)] wherein $(x)_p = \frac{\Gamma(x+p)}{\Gamma(p)}$ is the Pochhammer number [17].

The different classical fading models are included in the generalized κ − μ shadowed fading model as distinctive cases, such as, Rician shadowed, κ − μ, Rician, Rayleigh, and Nakagami-m̂ fading model. With different set of parameters, these classical fading models can be obtained as distinctive cases [15][16]. We summarized in Table 1, herein, m_ℓ and K_ℓ, respectively, represent the Nakagami-m̂ and the Rician fading parameters.

Table 1: Special cases of the κ − μ shadowed distribution [15] [17]

Fading Distribution	κ	μ	m
$\kappa-\mu$	κ	μ	$m\to\infty$
Rician shadowed	$\kappa = K$	$\mu = 1$	$m \to m$
Rician	$\kappa = K$	$\mu = 1$	$m\to\infty$
Nakagami-m̂	$\kappa \to 0$	$\mu = \hat{m}$	$m\to\infty$
Rayleigh	$\kappa \to 0$	$\mu = 1$	$m\to\infty$

3. Average Capacity and Throughput Analysis

In this section, the exact analytical expression for the average capacity is first derived, and, based on the derived average capacity expression, a new and exact expression for the achievable throughput is subsequently obtained.

3.1 Average Capacity Analysis

The average capacity is the statistical mean of the mutual information between the source and destination. In a DF relay system, the average capacity of the considered system can be determined by (9), for which the minimum values of the first-hop average capacity $\overline{C}_R$ and the second-hop average capacity $\overline{C}_D$ are used [7, eq. (17)].

$$\overline{C} = \min(\overline{C}_R, \overline{C}_D) \tag{9}$$

where $\overline{C}_R = \frac{1}{2}E[\log_2(1+\gamma_R)]$, $\overline{C}_D = \frac{1}{2}E[\log_2(1+\gamma_D)]$, and $E[\cdot]$ is the expectation operator. By using (5) and (8), the following equation can be derived:

$$\overline{C}_R = \sum_{n=0}^{\infty} \frac{\xi_1 (N_1 m_1)_n \delta_1^n \theta^{N_1\mu_1+n}}{n!(N_1\mu_1)_n \ln(2)} \int_0^\infty \frac{\ln(1+\gamma)\gamma^{N_1\mu_1+n-1}}{e^{-\theta\psi_1\gamma}} \tag{10}$$

where $\theta = \frac{P_s d_1^{-\alpha}(1-\rho)}{(1-\rho)\sigma_{a,r}^2 + \sigma_{c,r}^2}$. According to [18, eq. (8.4.6.5)], $\ln(1+\gamma)$ can be represented in terms of Meijer G-function as

$$\ln(1+\gamma) = G_{2,2}^{1,2}\left[\gamma \,\middle|\, {}^{1,\ \ 1}_{1,\ \ 0}\right] \tag{11}$$

where $G_{\cdot,\cdot}^{\cdot,\cdot}[\cdot\,|\,\cdot]$ is the Meijer-G function [17, eq. (9.301)]. Then, by combining (10) and (11), and using the integral identity [17, eq. (7.813.1)], $\overline{C}_R$ is derived as

$$\overline{C}_R = \sum_{n=0}^{\infty} \frac{\xi_1 (N_1 m_1)_n \delta_1^n \psi_1^{-N_1\mu_1-n}}{n!(N_1\mu_1)_n \ln(2)} \times G_{3,2}^{1,3}\left[\frac{1}{\theta\psi_1} \,\middle|\, {}^{1-N_1\mu_1-n,\ \ 1\ \ 1}_{1\ \ \ \ 0}\right]. \tag{12}$$

To derive $\overline{C}_D$, the PDF of γ_D from (7) is first obtained, as follows:

$$f_{\gamma_D}(\gamma) = \int_0^\infty \frac{1}{x} f_{\gamma_{\|\mathbf{h}_1\|^2}}(x) f_{\gamma_{\|h_2\|^2}}\left(\frac{b\gamma}{x}\right) dx \tag{13}$$

where $\varphi = \frac{\eta\rho P_s}{d_1^\alpha d_2^\alpha(\sigma_{a,d}^2 + \sigma_{c,d}^2)}$, and $f_{\|h_1\|^2}(\gamma)$ and $f_{\|h_2\|^2}(x)$ are given by (8). By using the integral identity [17, eq. (3.471.9)], the following equation is derived:

$$f_{\gamma_D}(\gamma) = \sum_n^\infty \sum_{i=0}^\infty \frac{2\xi_1\xi_2 (N_1 m_1)_n (N_2 m_2)_i \delta_1^n (\varphi\delta_2)^i}{n!i!(N_1\mu_1)_n (N_2\mu_2)_i} \times \gamma^{\frac{N_1\mu_1+N_2\mu_2+i-2}{2}} \left(\frac{\varphi\psi_2}{\psi_1}\right)^{\frac{N_1\mu_1-N_2\mu_2+n-i}{2}} \times K_{N_1\mu_1-N_2\mu_2+n-i}\left(2\sqrt{\varphi\psi_1\psi_2\gamma}\right) d\gamma \tag{14}$$

where $K_v(\cdot)$ is the v-th order modified Bessel function of the second kind [17]. From (14), we get

$$\overline{C}_D = \sum_n^\infty \sum_{i=0}^\infty \frac{2(N_1 m_1)_n (N_2 m_2)_i}{n!i!(N_1\mu_1)_n (N_2\mu_2)_i} \left(\frac{\varphi\psi_2}{\psi_1}\right)^{\frac{N_1\mu_1-N_2\mu_2+n-i}{2}} \times \frac{\xi_1\xi_2\varphi^{N_2\mu_2}\delta_1^n(\varphi\delta_2)^i}{\ln(2)} \int_0^\infty \ln(1+\gamma)\gamma^{\frac{N_1\mu_1+N_2\mu_2+i-2}{2}} \times K_{N_1\mu_1-N_2\mu_2+n-i}\left(2\sqrt{\varphi\psi_1\psi_2\gamma}\right) d\gamma. \tag{15}$$

The modified Bessel function in (15) can be expressed as [18, eq. 8.4.23.1]

$$K_V(2\sqrt{x}) = \frac{1}{2} G_{0,2}^{2,0}\left[x \,\middle|\, {}^{\cdot,\ \ \cdot}_{V/2,\ \ -V/2}\right]. \tag{16}$$

By using (11), (16), and integral relationship [19, eq. (21)], the following equation is derived:

$$\overline{C}_D = \sum_n^\infty \sum_{i=0}^\infty \frac{2(N_1 m_1)_n (N_2 m_2)_i}{n!i!(N_1\mu_1)_n (N_2\mu_2)_i} \left(\frac{\varphi\psi_2}{\psi_1}\right)^{\frac{N_1\mu_1-N_2\mu_2+n-i}{2}} \times \frac{\xi_1\xi_2\varphi^{N_2\mu_2}\delta_1^n(\varphi\delta_2)^i}{\ln(2)} \times G_{2,4}^{3,1}\left[\varphi\psi_1\psi_2 \,\middle|\, {}^{\cdot,\ \ \cdot}_{1-N_1\mu_1+n,\ \ 1-N_2\mu_2+i}\right]. \tag{17}$$

3.2 Throughput Analysis

In the delay-tolerant transmission mode, the throughput τ of the considered system at the destination node can be given by [6]

$$\tau = \frac{T/2}{T}\overline{C} = \frac{1}{2}\min\{\overline{C}_R, \overline{C}_D\}. \tag{18}$$

The optimal power splitting ratio ρ^* and the optimal throughput τ^* is desirable to obtain for a given set of parameters.

4. Special Cases

The $\kappa-\mu$ shadowed fading model encompasses $\kappa-\mu$, Rician, Rician shadowed, Rayleigh, and Nakagami-$\hat{m}$ as distinctive cases. Therefore, the exact analytical expressions for the average capacity and throughput for different shadowing and fading scenarios can be find from the derived results. These results are not shown here for the sake of brevity, and can be obtain using (9) and (18) with the help of table 1.

5. Numerical Results and Discussion

In this section, we analyze the system performance of a DF relaying system with beamforming under $\kappa-\mu$ shadowed fading environment where an energy-constrained relay harvests energy from the source signal. The power splitting ratio can be optimized to achieve maximum throughput for a given parameter set. However, in this section, we focus only on investigating the performance of our considered system for different number of antennas and for different values of the fading and shadowing parameters.

Unless otherwise stated, some system parameters are set as follows: the source transmit power, $P_s = 1\,\mathrm{W}$, energy-conversion efficiency, $\eta = 1$, path-loss exponent, $\alpha = 2.7$; distances are normalized to unity, $d_1 = d_2 = 1$; and average channel gains, $\lambda_1 = \lambda_2 = 1$. For simplicity, the similar noise variances at the relay and each antenna of the destination are set as $\sigma_{a,r}^2 = \sigma_{c,r}^2 = 0.01$ and $\sigma_{a,d}^2 = \sigma_{c,d}^2 = 0.01$, respectively. The values of ρ is taken from 0.1 to 0.9 with a step size of 0.1. The analytical expressions (9) and (18) containing infinite series are evaluated to achieve sufficient accuracy for all cases considered in this paper by truncating infinite sums to first 50 terms.

Fig. 2 shows the throughput, τ, versus power splitting ratio, ρ, for various channel models; such as, $\kappa-\mu/\kappa-\mu$, Rician shadowed/Rician shadowed, the $\kappa-\mu$ shadowed $/\kappa-\mu$ shadowed, Nakagami-$\hat{m}$ / Nakagami-$\hat{m}$, and Rician/Rician fading models. These results are obtained as particular cases from the obtained anaytical expressions over $\kappa-\mu$ shadowed fading channels. The excellent agreement between the exact analytical and simulated results verifies the validity of the analysis for the classical fading channels. The throughput, τ, improves as power splitting ratio, ρ, increases from 0 to an optimal value, ρ^*, and the throughput decreases as the ρ increases from its optimal value to 1.

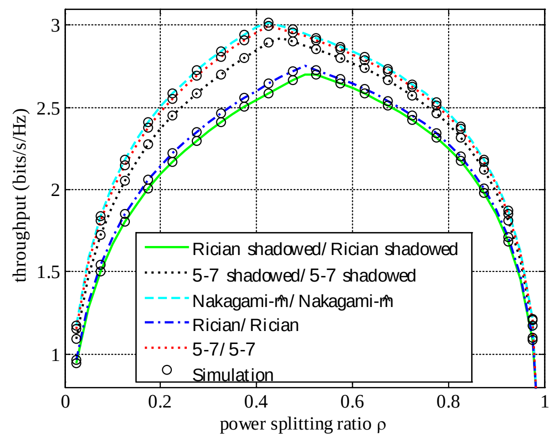

Fig. 2 Throughput versus power splitting ratio for various channel models: the $\kappa-\mu$ shadowed/ $\kappa-\mu$ shadowed $(\kappa_1=\kappa_2=10$, $\mu_1=\mu_2=2$, and $m_1=m_2=0.5)$, $\kappa-\mu$ / $\kappa-\mu$ $(\kappa_1=\kappa_2=10$ and $\mu_1=\mu_2=3)$, Rician shadowed/Rician shadowed $(K_1=K_2=10$ and $m_1=m_2=0.5)$, Rician/Rician $(K_1=K_2=5)$, and Nakagami-$\hat{m}$ /Nakagami-$\hat{m}$ $(m_1=m_2=2)$ fading links when $N_1=N_2=2$.

Fig. 3 shows the throughput performance versus the power splitting ratio for different number of antennas in $\kappa-\mu$ shadowed fading environment; here, the throughput improves as the number of antennas increases. Also, in Fig. 3, throughput performance is cross-compared under various antenna configurations at the source and destination. The cases with $N_1 > N_2$ and $N_1 < N_2$ were analyzed, and the observations show that a large number of antennas at the source (i.e., $N_1 > N_2$) provides a higher throughput gain compared with a large number of antennas at the destination (i.e., $N_1 < N_2$); this is because the source with transmit beamforming transfers the energy in a narrow beam towards the relay. As a result, the relay harvests a great deal of energy to forward the decoded signal to the destination.

Figs. 4 and 5 show the throughput performance versus the power splitting ratio for different number of antennas when the same fading conditions are assumed for both links (i.e., identical channels). In Fig. 4, we observe that the throughput improves as the number of source antennas increases but the optimal value ρ^* remains constant (i.e., $\rho^* = 0.65$) for all number of the source antennas. On the other hand, in Fig. 5, it is observed that the throughput improves and ρ^* becomes smaller as the number of destination antennas increases, for example, when the number of antennas are set as $N_1{=}N_2{=}1$, the maximal throughput is obtained when $\rho^* = 0.65$, while for $N_1{=}1$ and $N_2{=}\ 2$, maximal throughput occurs at $\rho^* = 0.425$, and so on.

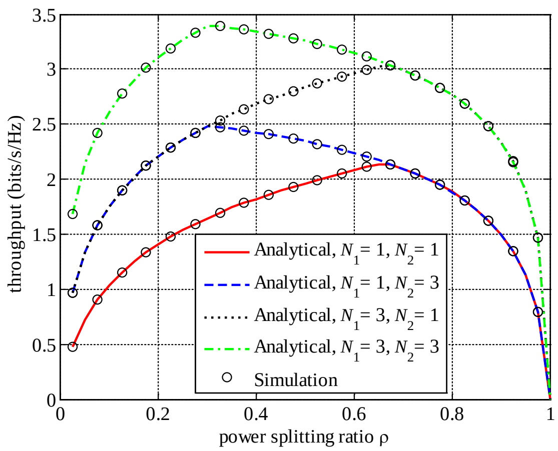

Fig. 3 Throughput for different number of antennas at source when $\kappa_1 = \kappa_2 = 1$, $\mu_1 = \mu_2 = 2$, and $m_1 = m_2 = 0.5$.

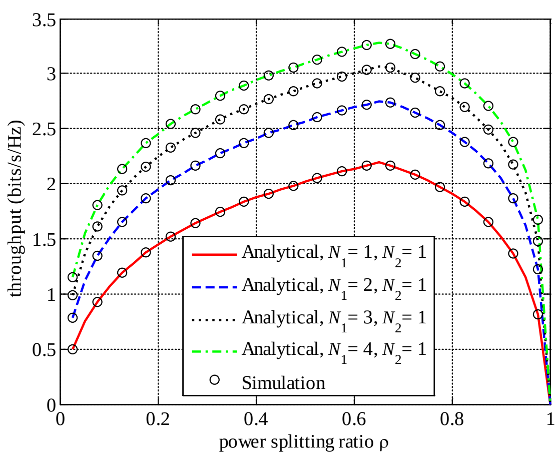

Fig. 4 Throughput versus power splitting ratio for different number of antennas when $\kappa_1 = \kappa_2 = 1$, $\mu_1 = \mu_2 = 2$, and $m_1 = m_2 = 0.5$.

6. Conclusion

We studied the energy harvesting in a DF relaying system with beamforming based on the PSR protocol over $\kappa - \mu$ shadowed fading channels. We derived the exact analytical expressions for the average capacity and throughput under various symmetric and asymmetric shadowing and fading conditions. We analyzed the system performance for different set of parameters. It is concluded that the system performance improves with increasing number of antennas at the source as compared to increasing the number of antennas at the destinaiton. It is also observed that the system performance is decreased with increasing shadowing parameters in LoS (line-of-sight) conditions.

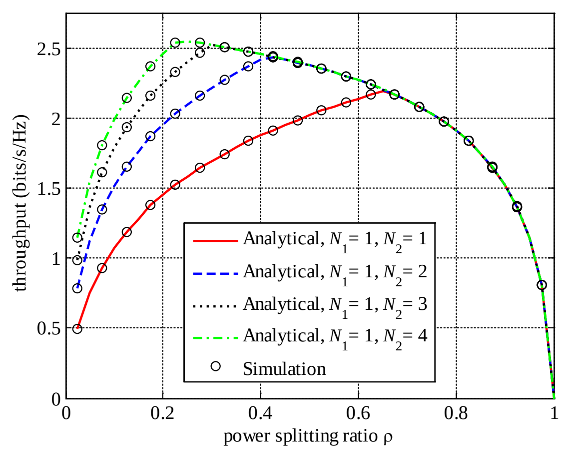

Fig. 5 Throughput for different numbers of antennas at destination when $\kappa_1 = \kappa_2 = 0.5$, $\mu_1 = \mu_2 = 2$, and $m_1 = m_2 = 0.5$.

Acknowledgements

This research is funded by R&D, Balochistan University of Engineering and Technology, Khuzdar, Pakistan.

References

[1] Sudevalayam, S., and Kulkarni, P.: Energy harvesting sensor nodes: survey and implications, IEEE Commun. Surveys Tuts., 13(3), pp. 443–461, Third Quart. 2011.

[2] Li, W., Ku, M. L., Chen, Y,. Liu, K. J. R.: On outage probability for two-way relay networks with stochastic energy harvesting, IEEE Trans. Commun., 64(5), pp. 1901–1915, May 2016.

[3] Lu, X,. Wang, P., Niyato, D., Kim, D. I., Han, Z,: Wireless networks with RF energy harvesting: A contemporary survey, IEEE Commun. Surveys Tuts., 17(2), pp. 757–789, Second Quart. 2015.

[4] Nasir, A. A., Zhou, X., Durrani, S., Kennedy, R. A.: Relaying protocols for wireless energy harvesting and information processing, IEEE Trans. Wirel. Commun., 2(7), pp. 3622–3635, Jun. 2013.

[5] Wang, X., Liu, J., Zhai, C., Ma, S., Wang, W.: Energy efficiency relay networks with wireless power transfer from a multi-antenna base station, Trans. Emerging Tel. Technol., 27(4), pp. 533–543, Sep. 2016.

[6] Nasir, A. A., Zhou, X., Durrani, S., Kennedy, R. A.: Throughput and ergodic capacity of wireless energy harvesting based DF relaying network, Proc. of IEEE ICC pp. 4066-4071, Jun. 2014.

[7] Gu, Y., Aïssa, S.: RF-based energy harvesting in decode-and-forward relaying systems: ergodic and outage capacities, IEEE Trans. Wirel. Commun., 14(11), pp. 6425–6434, Nov. 2015.
[8] Ishibashi, K.: Dynamic harvest-and-forward: new cooperative diversity with RF energy harvesting, Proc. of IEEE Wireless Commun. Signal Process., pp. 1-5, Oct, 2014.
[9] Do., N. T., Bao., V. N. Q., An. B.: Outage performance analysis of relay selection schemes in wireless energy harvesting cooperative networks over non-identical rayleigh fading channels, Sensors, 16(3), pp. 1–16, Feb. 2016.
[10] Ding. Z., Krikidis, I., Sharif, B., Poor, H. V.: Wireless information and power transfer in cooperative networks with spatially random relays, IEEE Trans. Wirel. Commun., 13(8), pp. 4440–4453, Aug. 2014.
[11] Krikidis, I.: Relay selection in wireless powered cooperative networks with energy storage devices, IEEE J. Selec. areas on Commun., 33(12), pp. 2596–2610, Dec. 2015.
[12] Hoang, T. M., Duy, T. T., Bao, V. N. Q.: On the performance of non-linear wirelessly powered partial relay selection networks over Rayleigh fading channels, Proc. of IEEE 3rd National Foundation for Sc. and Technol. Development Conf. on Inform. and Comput. Sc., pp.6-11, Sep. 2016.
[13] Badarneh OS, Almehmadi FS, Ansari IS, Yang X.: Wireless energy harvesting in cooperative decode-and-forward relaying networks over mixed generalized $\eta-\mu$ and $\kappa-\mu$ fading channels. Trans Emerg Tel. Technol. DOI: 10.1002/ett.3262: pp.1–18, 2017.
[14] Hussain, A., Kim, S.-H., Chang, S.-H.: Non-linear energy harvesting relaying with beamforming and hardware impairments in $\kappa-\mu$ shadowed fading environment, Trans. Emerg. Tel. Technol., 2018.
[15] Hussain, A., Kim, S.-H., Chang, S.-H.: Dual-hop variable-gain AF relaying with beamforming over $\kappa-\mu$ shadowed fading channels, Proc. of IEEE GLOBECOM, pp. 1–6, 2016.
[16] Pairs, J. F.: Statistical characterization of $\kappa-\mu$ shadowed fading, IEEE Trans. Veh. Technol., 63(2), pp. 518–526, Feb. 2014.
[17] Gradshteyn, I. S., Ryzhik, I. M., Table of integrals, series, and products. 7th ed. San Diego, CA, USA: Academic, 2007.
[18] Prudnikov, A. P., Brychkov, Y. A., Marichev, O. I.: Integrals and series. Gordon and Breach Science, Vol. 3, 1986.
[19] Adamchik, V. S., Marichev, O. I., The algorithm for calculating integrals of hypergeometric type functions and its realization in reduce systems, Proc. of Int. Symp. Symbolic and Algebraic Computation, pp. 212–224, Aug. 1990.

Ayaz Hussain received the B.Sc. in Telecommunication Engineering from Mehran University of Engineering and Technology, Jamshoro, Pakistan, in 2006 and the M.Sc. in Electronic and Electrical Engineering from Hanyang University, ansan, Korea in 2010. Currently, he received Ph.D. degree in Electrical and Computer Engineering from Sungkyunkwan University, Suwon, Korea in 2018. His research interests include wireless communication systems; in particular, cooperative relaying, MIMO technology, D2D communications, and energy harvesting.

Inayat Ali received the B.E. degree in electronics engineering in 2009 and M.E. degree in telecommunication engineering in 2011, from PAF-KIET and Hamdard University, Karachi, Pakistan, respectively. He is currently pursuing the Ph.D. degree in information and communication engineering from Sungkyunkwan University, Suwon, Korea. His research interests include LDPC codes, SC LDPC codes, modern coding theory, and information theory.

Zahoor Ahmed received his PhD in Telecommunication Engineering from Universite de Limoges France in 2011 and ME in Computer Information System Engineering from UET Peshawar, Pakistan in 2004. He has done his BE in Electrical Engineering from Balochistan UET Khuzdar in 1995. He holds over 17 years of research and teaching experience in BUET Khuzdar at the level of Professor. His area of interest is Space time coding and cooperative relay network communication system.

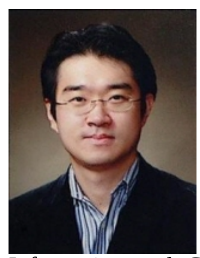

Sang-Hyo Kim received the B.Sc., M.Sc., and Ph.D. in Electrical Engineering from Seoul National University, Seoul, Korea in 1998, 2000, and 2004, respectively. From 2004 to 2006, he had been a Senior Engineer at Samsung Electronics. He visited University of Southern California as a visiting scholar from 2006 and 2007. In 2007, he joined the College of Information and Communication Engineering, Sungkyunkwan University, Suwon, Korea, where he is currently an Associate Professor. In 2015, he visited University of California San Diego. He has served as an editor for the Transactions on Emerging Telecommunications Technologies and the Journal of Communications and Networks from 2013. His research interests include coding theory, wireless communications, signal design, and secure communications.